Detection of subsurface rocks in sand of similar composition using a millimeter wave imaging system

Todd Du Bosq · Robert Knox · Glenn Boreman

Abstract The ability to image objects, whether natural or man made, beneath soil is extremely beneficial. The detection scenario becomes increasingly difficult when the object and the soil are composed of the same material, as in the detection of subsurface rocks. The feasibility of detecting rock in similar composition is explored. An active multi-spectral millimeter wave (mmW) imaging system operating from 90–140 GHz is used to detect lava rock buried beneath lava sand at various depths, up to a limit of 64 mm. The principal component analysis method was used in the data processing.

1 Introduction

The detection of subsurface anomalies is a topic of considerable interest in planetary exploration and military applications. The feasibility of detecting rocks beneath the loose soil on Mars composed of the same material will allow vehicles such as the Mars rover to safely navigate around areas where the soft soil can potentially trap the vehicle [1, 2]. The Mars rover Opportunity has been trapped multiple times in loose soil before slowly maneuvering its way free [3]. Unmanned ground vehicles are also useful for high-risk military zones such as mine fields where soft terrain can potentially trap the vehicle [4]. Avoiding these traps will save time, resources, and possibly the vehicle. The ability to detect buried rocks will depend on soil transmission and scattering. Soils with particle sizes larger than the wavelength have low transmittance due to scattering [5]. A multi-spectral millimeter wave (mmW) imaging system used to penetrate the soil and detect the buried

T. Du Bosq · G. Boreman (✉)
CREOL–College of Optics and Photonics, University of Central Florida, 4000 Central Florida Blvd,
Orlando, FL 32816, USA
e-mail: boreman@creol.ucf.edu

R. Knox
Epsilon Lambda Electronics Corp., 396 Fenton Lane, Suite 601, West Chicago, IL60134, USA

rock is demonstrated. The mmW imager operates from 90–140 GHz. Some advantages of a higher frequency imaging system, compared to current ground penetrating radar systems, is that it will allow for a potentially more compact and higher resolution system. This mmW imager system has been previously demonstrated to detect buried plastic landmines [6]. The information provided by the multi-spectral images is analyzed through a principal component analysis (PCA) image processing method. With this procedure, structural information contained in each frequency frame of the multi-spectral image is condensed into a single image and the buried object can be located. There is no material difference between the soil and the rock producing a difficult detection scenario. The difference in the density of the rock compared to the soil is determined using the PCA method. This paper presents the sample preparation, experimental setup for the mmW imaging system, the signal processing method used, and imaging results for the detection of subsurface density anomalies.

2 Sample preparation

To simulate the soil and rocks found on Mars, a bag of lava rocks (Red Volcanic Moon Rocks®) was procured commercially. The larger lava rocks were set aside to be used as Mars rock samples. The remaining rocks were hand crushed using an aluminum pipe and a piston-like handle into lava sand. The pulverized sand was sieved, removing all particles larger than 1 mm, giving particle sizes similar to those found in other Mars test beds [7]. Most of the particles were a fine dust, but some were as big as 1 mm. The soil and the rocks were then baked in an oven at 135 degrees C for over 24 hours to remove the moisture. The densities of the lava rock and lava soil were measured as described in [8]. The lava rock has a density of 1.646 g/cm^3 and the lava soil has a density of 1.325 g/cm^3.

3 Imaging setup

The mmW imaging system uses an Anritsu vector network analyzer (VNA) operating from 90–140 GHz as the source and detector. The power emitted from the VNA ranges from 0.2 mW to 2 mW throughout the 90–140 GHz band. The VNA modules, equipped with 16 degree horn antennas, were mounted on a vertically oriented optical table, shown in Fig. 1, right. Manual translation stages were added to the VNA modules to allow adjustment of the imager height. The mmW radiation was focused through a set of high density polyethylene (HDPE) lenses onto the sample and then reflected back through another set of HDPE lenses into the VNA receiver. The focal length for both lens assemblies was 140 mm, with a diameter of 50.8 mm. The image-plane resolution spot size was about 20 mm, with a depth of focus about 60 mm. Two motorized translation stages, with 200 mm maximum travel distance and 50 mm/s maximum velocity, were mounted perpendicular to each other. The sample was attached to the stages using a long aluminum arm. The aluminum platform at the end of the arm which held the sample was a square annulus, covered by a thin sheet of gypsum board, which avoided a highly reflecting metallic plane directly underneath the sample. The lava rock about 30 mm by 60 mm dimension was placed in an 180 mm × 180 mm × 220 mm container surrounded by the lava soil, as seen in Fig. 1, left.

A broadband convoluted foam millimeter wave absorber, ECCOSORB CV, was placed under the sample to eliminate back reflections from the optical table. A program was written in LABVIEW to capture a raster scan image (Fig. 1 inset), containing 37 lines, of

Fig. 1 (Left) Photograph of the lava rock before being covered by lava sand. (Right) Photograph of the active multi-spectral 90–140 GHz mmW imaging system. (Inset) Schematic of the path for taking a raster scan image.
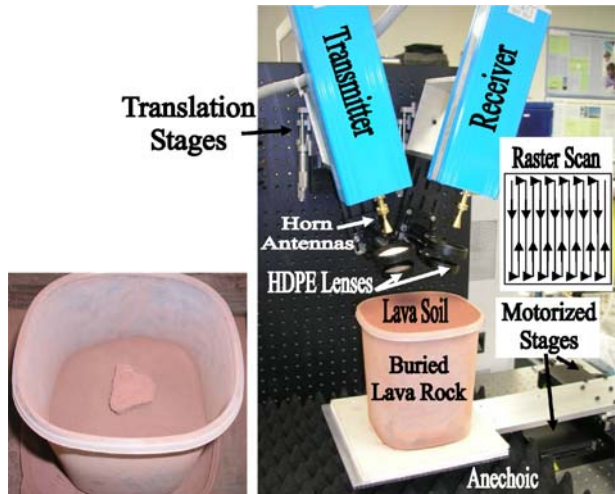
the lava rock under the soil. At each position of the scan, the VNA measured the reflected power, spectrally resolved from 90–140 GHz in 1 GHz steps. The resulting data set was converted into a set of images (one for each frequency used) by a MATLAB software program. In our case, the total number of frequencies is 51. The images taken were 180 mm × 180 mm with a 5 mm step size. The entire scan took about 7 minutes to complete, including the mechanical settling time at each step. In this development, we used only the reflection amplitude information. Phase information was also available from the VNA, but with the small density differences between target and background in this study, we did not find appreciable benefit by including phase information.

4 Signal processing

The initial data set is a collection of the 51 images, corresponding to the mmW frequencies from 90–140 GHz in 1 GHz steps. The information about the structure of the object is not concentrated around a single frequency but spread over the frequency spectrum. Therefore, it is necessary to employ a method that can combine the majority of the available information into a single image with a high signal to noise ratio.

For this purpose, we have used a principal component analysis (PCA) method. PCA is a multivariate statistical method primarily developed to deal with a large ensemble of observations of N random variables described in [9].

Normally, the principal features of the data set are well represented by a small number of principal components [10]. This allows the main principal components to be selected and then to reconstruct the original images using only them, filtering out the higher components. This process is called rectification [11]. A statistical analysis of the principal component decomposition enables the classification and grouping of the eigenvalues and the corresponding eigenimages into processes. A subset of eigenvalues is considered to belong to the same process when the variation of successive eigenvalues is within the measurement uncertainty. The uncertainty is produced by the finite size of the data set and the high-order cumulants of the underlying probability distribution [11]. A process is defined as a set of frames containing a sequential subset of principal components. These

processes could contain a single principal component or a large number of them. Figure 2 shows the application of the PCA to a set of 51 single frequency images of the lava rock. The components are grouped into two processes: the lowest order component process and the higher components process. The lowest order component process is dominated by the reflection from the soil surface. The standard deviation image of this component process has very little contrast and the lava rock can not be seen. The reflections from the lava rock are small compared to the lowest order component but can be seen in the higher components process using the PCA method. The higher components process is used in the detection of the lava rock in the results to follow.

5 Results

The mmW imaging system measured the lava rock buried in lava sand at various depths. The rocks were buried at depths of 5 mm, 15 mm, 25 mm, 38 mm, 50 mm, and 64 mm. In Fig. 3, images of the lava rock buried 5 mm deep (left) and 38 mm deep (right) in sand are shown.

The signal-to-noise ratio (SNR) was determined for each image, where the signal is the reflection from the rock and the noise is the reflection from the surrounding soil. The plot of SNR vs. rock depth is shown in Fig. 4. As expected the SNR decreases with increased depth. The SNR of the rock buried deeper than 64 mm approaches 0 dB and can not be located from the surrounding soil. The reflected signal varies exponentially with soil depth according to $|E_{ret}|=|E_{in}|$ exp$[-\alpha 2x]$, where α is the attenuation due to scattering and x is the depth of the rock. An exponential fit of the experimental data gives a value of α of 0.0113 mm^{-1} for lava soil with an R^2 value of 0.92.

6 Conclusions

A 90–140 GHz mmW imaging system demonstrated the ability to detect lava rock buried beneath lava sand at various depths. The principal component analysis method was applied

Fig. 2 Application of the PCA to a set of 51 single frequency images of the lava rock. The components are grouped into 2 processes. The buried lava rock is detected using the higher components process.
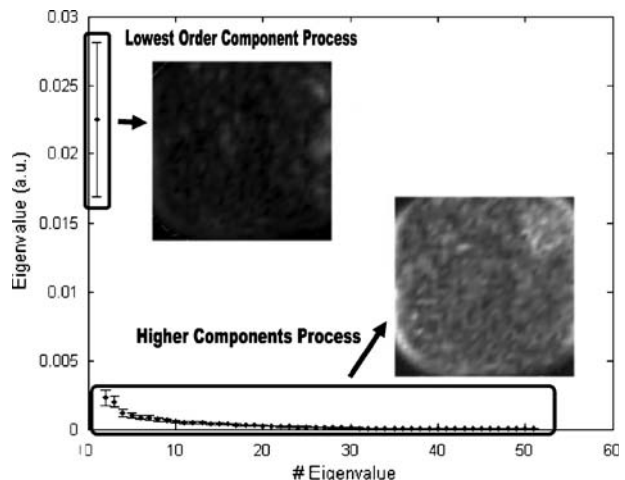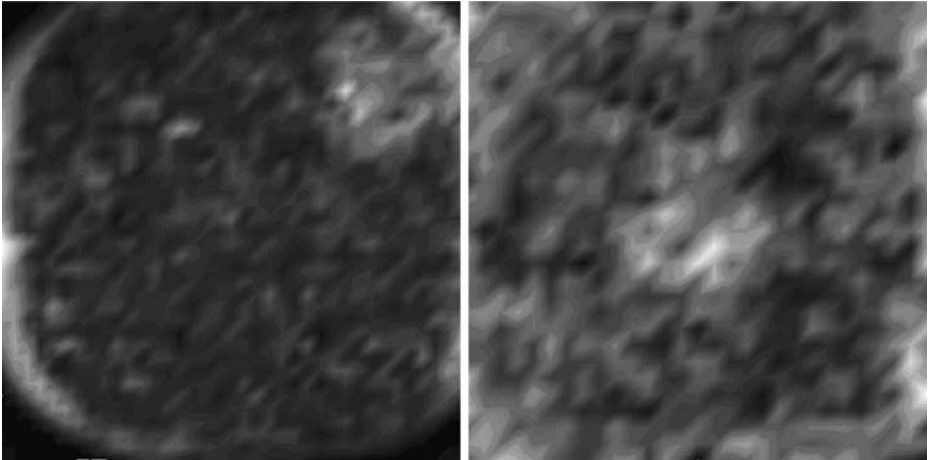
Fig. 3 Left: Higher order process image of the lava rock (upper right corner) buried 5 mm deep in lava sand. The image is 180 mm x 180 mm with a step size of 5 mm. Right: Higher order process image of the lava rock (center) buried 38 mm deep in lava sand. The image is 140 mm x 140 mm with a step size of 5 mm.

to the 51 frames to help locate the lava rock beneath the soil. The rock was located in the higher order process image up to 64 mm beneath the surface. After 64 mm, the rock could not be distinguished from its surroundings with a SNR close to 0 dB. An increase in power beyond the 0.2 to 2 mW used would be needed to penetrate further into the sand. Also, the diffraction limited spot size of a 50.8 mm diameter lens with a focal length of 140 mm is large compared to the size of the rock used as our object somewhat decreasing the detection probability but giving a significant depth of focus. With increased power and aperture size, the detection of larger lava rocks beneath lava soil at greater depths is promising in the 90–140 GHz range. An unmanned ground vehicle equipped with a 90–140 GHz imaging system will have the capability to avoid potentially hazardous terrain. Further investigation is required to determine the performance of the system in the presence of multiple rocks of different sizes and proximity.

Fig. 4 SNR versus rock depth.
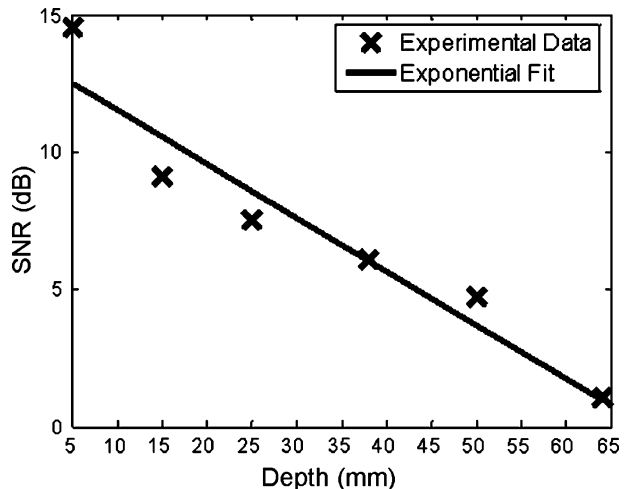
References

1. B. H. Wilcox, Proc. SPIE **4715**, 267 (2002).
2. G. Reina, L. Ojeda, A. Milella, and J. Borenstein, IEEE/ASME Trans. Mechatron **11**, 185 (2006).
3. Associated Press,"Stuck for a month, Mars Rover finally gets back on track," *New York Times*, Retrieved April 21, 2008, from http://www.nytimes. com/2005/06/06/science/06mars.html, (2005).
4. S. Wasson, J. Guilberto, W. Ogg, K. Wedeward, S. Bruder, and A. El-Osery, Proc. SPIE **5415**, 1231 (2004).
5. T. W. Du Bosq, R. E. Peale, A. Weeks, J. Grantham, D. Dillery, D. Lee, D. Muh, and G. Boreman, Proc. SPIE **5790**, 66 (2005).
6. T. W. Du Bosq, J. M. Lopez-Alonso, and G. D. Boreman, "Millimeter wave imaging system for landmine detection," Appl. Optics **45**, 5686 (2006).
7. H. A. Perko, J. D. Nelson, and J. R. Green, J. Aerospace Eng. **19**, 169 (2006).
8. G. Balco and J. O. Stone, "Measuring the density of rock, sand, till, *etc.*" *UW Cosmogenic Nuclide Laboratory, methods and procedures*, Retrieved April 21, 2008, from http://depts.washington.edu/cosmolab/chem.html, (2003).
9. D. F. Morrison, *Multivariate statistical methods*, 3rd edn. (McGraw-Hill, Singapore, 1990).
10. J. Kositsky, R. Cosgrove, C. Amazeen, and P. Milanfar, Proc. SPIE **4742**, 206 (2002).
11. J. M. Lopez-Alonso, J. Alda, and E. Bernabeu, Appl. Optics **41**, 320 (2002).